Contribution from the Department of Chemistry,
University of Rhode Island, Kingston, Rhode Island 02881

Madelung Energy Calculations on the Highly Conducting Molecular Metal Nickel Phthalocyanine Iodide

WILLIAM B. EULER

Received September 26, 1983

The Madelung energy of the one-dimensional molecular metal NiPcI is calculated as a function of charge transfer and stacking motif along the unique axis. The partial ionicity along the conducting stack is modeled by both uniform, delocalized charges (Hartree–Fock limit) and distributed, localized charges (Wigner limit). It is found that the Madelung energy is minimized at the integral oxidation state $\rho = 1$ for the Hartree–Fock limit, whereas the Wigner limit is minimum for nonintegral ρ. The most negative Madelung energy is found in the Wigner limit, but only when the anion and cation stacks are highly correlated is there sufficient Madelung energy to balance the energetic cost of charge transfer. The macromolecular stacking axis of NiPcI has alternate rings rotated by 39.5°; however, Madelung energy calculations show that a rotation angle of 0° would be 0.1–0.2 eV/molecule more stable. The observed rotation angle arises from a balance of a variety of forces.

Introduction

The use of metallomacrocycles as donors in highly conducting one-dimensional donor–acceptor complexes has led to a variety of interesting and novel materials.[1] The most extensive studies on these types of compounds have been of metalloporphyrin and metallophthalocyanine iodides,[2] primarily because they possess ideal geometric and electronic characteristics and are readily available. These macrocycles are planar and consequently easily form stacks leading to one-dimensional behavior. The ligands have extensive delocalized π systems that permit good overlap between molecules along the stack. Moreover, nearly every element in the periodic table can be put into the core of either of these macrocycles,[3] thus, a wide variety of small perturbations to the ligand π system can be achieved.

The most extensively characterized phthalocyanine-based molecular metal is nickel phthalocyanine iodide (NiPcI).[1a,4] The crystal structure of this material shows that the metallophthalocyanine forms extended, yet segregated, stacks with alternate macrocycles rotated by 39.5° and iodine atoms filling the channels created between these stacks. Analysis of ^{129}I Mössbauer and resonance Raman spectra led to the conclusion that the iodine is exclusively in the form of triiodide, so that the proper formulation for this substance is $(NiPc^{\rho+})(I_3^-)_\rho$, where $\rho = {}^1/_3$. Electrical conductivity studies showed that NiPcI has a high room-temperature conductivity, $\sigma \sim 500\ \Omega^{-1}\ cm^{-1}$, with a metallic temperature dependence, $d\sigma/dT <$ 0, down to ~20 K where the conductivity reaches a maximum and then decreases to about the room-temperature value as the temperature approaches 100 mK.[4a] Electron paramagnetic resonance spectra showed that the charge carrier is associated with ligand π orbitals. Finally, a solid-state electrochemical study measured the ΔG of formation for NiPcI (from NiPc and I_2) to be −2.1 kcal/mol,[4b] indicating the shallow energy minimum associated with charge transfer. The thermochemical data also enabled the calculation of the crystal lattice enthalpy for NiPcI, $H_{lat} = -109$ kcal/mol.

This paper reports on the calculation of the Madelung energy for NiPcI in an attempt to account for the observed lattice enthalpy. Madelung energy calculations have been done for a number of organic donor–acceptor complexes[5] with mixed results. For example, the Madelung energy accounts for more than 90% of the lattice energy in $TTFI_{0.71}$[5f] (TTF = tetrathiafulvalene) but only about 30% of the lattice energy in TTF-TCNQ[5d] (TCNQ = tetracyanoquinodimethane), both good one-dimensional conductors like NiPcI. Proper calculation of the Madelung energy depends in large part upon the choice of charge model employed.[6] Most frequently the fractional point charge approximation is used; in this scheme, each atom is assigned a fractional charge, usually found by some sort of population analysis from an appropriate quantum-chemical calculation. In addition to charge distribution within the molecular species, the nonintegral oxidation state of these molecular metals requires that the charge distribution along the stack must also be considered. In the calculations reported here, the fractional point charge approximation is used, utilizing the Mulliken populations of the extended Hückel calculation of Schaffer et al.,[7] for NiPc. Both uniform charges (the Hartree–Fock limit) and localized charges (the Wigner limit) are used to model the charge distribution along the macrocyclic stack.

This report is concerned with two issues. First, what is the variation of the Madelung energy of NiPcI with the degree of charge transfer, and can the preference for $\rho = {}^1/_3$ be attributed to bulk Coulombic interactions? In the Hartree–Fock model the most stable lattice on the interval $0 < \rho < 1$

(1) (a) Ibers, J. A.; Pace, L. J.; Martinsen, J.; Hoffman, B. M. "Structure and Bonding"; Clark, M. J., et al., Eds.; Springer-Verlag: Berlin, 1982; Vol. 50. (b) Hoffman, B. M.; Martinsen, J.; Pace, L. J.; Ibers, J. A. "Extend Linear Chain Compounds"; Miller, J. S., Ed.; Plenum Press: New York, 1982; Vol. 3. (c) Cowie, M.; Gleizes, A.; Grynkewich, G. W.; Kalina, D. W.; McClure, M. S.; Scaringe, R. P.; Teitelbaum, R. C.; Ruby, S. L.; Ibers, J. A.; Kannewurf, C. R.; Marks, T. J. *J. Am. Chem. Soc.* **1979**, *101*, 2921. (d) Lin, L.-S.; Marks, T. J.; Kannewurf, C. R.; Lyding, J. W.; McClure, M. S.; Ratajack, M. T.; Whang, T.-C. *J. Chem. Soc., Chem. Commun.* **1980**, 954.

(2) (a) Schramm, C. J.; Scaringe, R. P.; Stojakovic, D. R.; Hoffman, B. M.; Ibers, J. A.; Marks, T. J. *J. Am. Chem. Soc.* **1980**, *102*, 6702. (b) Phillips, T. E.; Scaringe, R. P.; Hoffman, B. M.; Ibers, J. A. *Ibid.* **1980**, *102*, 3435. (c) Martinsen, J.; Pace, L. J.; Phillips, T. E.; Hoffman, B. M.; Ibers, J. A. *Ibid.* **1982**, *104*, 83. (d) Wright, S. K.; Schramm, C. J.; Phillips, T. E.; Scholler, D. M.; Hoffman, B. M. *Synth. Met.* **1979/1980**, *1*, 43. (e) Pace, L. J.; Martinsen, J.; Ulman, A.; Hoffman, B. M.; Ibers, J. A. *J. Am. Chem. Soc.* **1983**, *105*, 2612. (f) Diel, B. N.; Inabe, T.; Lyding, J. W.; Schoch, K. F., Jr.; Kannewurf, C. R.; Marks, T. J. *Ibid.* **1983**, *105*, 1551.

(3) Dolphin, D., Ed. "The Porphyrins"; Academic Press: New York, 1978.

(4) (a) Martinsen, J.; Greene, R. L.; Palmer, S. M.; Hoffman, B. M. *J. Am. Chem. Soc.* **1983**, *105*, 677. (b) Euler, W. B.; Melton, M. E.; Hoffman, B. M. *Ibid.* **1982**, *104*, 5966. (c) Inabe, T.; Kannewurf, C. R.; Lyding, J. W.; Moguel, M. K.; Marks, T. J. *Mol. Cryst. Liq. Cryst.* **1983**, *93*, 355.

(5) (a) Metzger, R. M. *J. Chem. Phys.* **1972**, *57*, 1870. (b) *Ibid.* **1972**, *57*, 1876. (c) *Ibid.* **1972**, *57*, 2218. (d) *Ibid.* **1981**, *75*, 3087. (e) Epstein, A. J.; Lipari, N. O.; Sandman, D. J.; Nielson, P. *Phys. Rev. B: Solid State* **1976**, *13*, 1569. (f) Torrance, J. B.; Silverman, B. D. *Ibid.* **1977**, *15*, 788. (g) Metzger, R. M.; Bloch, A. N. *J. Chem. Phys.* **1975**, *63*, 5098. (h) Metzger, R. M.; Arafat, E. S. *Ibid.* **1983**, *78*, 2696. (i) Metzger, R. M.; Arafat, E. S.; Kuo, C. S. *Ibid.* **1983**, *78*, 2706.

(6) Metzger, R. M. "The Physics and Chemistry of Low Dimensional Solids"; Alcacer, L., Ed.; D. Reidel Publishing Co.: Boston, 1980.

(7) Schaffer, A. M.; Gouterman, M.; Davidson, E. R. *Theor. Chim. Acta* **1973**, *30*, 9.

0020-1669/84/1323-2645$01.50/0

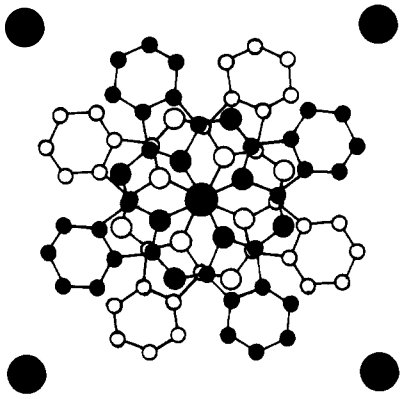

Figure 1. Structure of NiPcI as viewed down the stacking c axis. The large circles in the corners are iodine chains, while the Ni axis is in the center. Within the ligands, the smaller circles represent carbons and the larger circles represent nitrogens. Filled ligand atoms are at $z = 0$, while open ligand atoms are at $z = c/2$. Hydrogen atoms have been omitted for clarity.

is $\rho = 1$, whereas in the Wigner limit a nonintegral ρ gives a minimum in the Madelung energy. Second, is the observed angle of rotation between macrocycles along the chain axis favored by electrostatic energies? In all the cases studied here the favored angle is near 0°, not 40°; in fact, the observed packing arises from a balance of several different forces, with the geometric constraint of the size of the iodine channel apparently being the most important criterion.

Methodology

The Madelung energy, E^m, is found by the lattice sum (1) where q_i and q_j are the charges at sites i and j and r_{ij} is the distance between them; the sum is taken over all lattice sites. Two problems arise in

$$E^m = \sum_{i>}\sum_{j}(q_i q_j / r_{ij}) \qquad (1)$$

evaluating eq 1: the assignment of charges to the atoms in the molecular species and the slow convergence of the lattice summation. Several formulations have been used to accelerate convergence, most notably those of Evjen[8] and Ewald.[9] A computer program was written by using the latter procedure. In Ewald's method, an integral transformation is performed on the lattice sum of eq 1, and the resulting integral is divided into two portions. One portion is evaluated in direct space, while the other part is evaluated in reciprocal space. By careful selection of the cutoff parameter between the two integrals, the lattice sum of eq 1 can be evaluated by two rapidly, although conditionally, convergent lattice sums. Ample exposition of the mathematical details can be found elsewhere.[5a,10] In order to check convergence, different values of the cutoff parameter should give the same Madelung energy; in the results described here, the lattice sums were calculated to a convergence of at least 1 part in 10^4, which exceeds the precision of the input data.

Atomic coordinates are taken from the crystal structure of NiPcI reported by Schramm et al.[2a] This material crystallizes in the tetragonal cell $P4/mcc$, with two macrocycles per unit cell situated on sites of $4/m$ symmetry, as shown in Figure 1. There is a 39.5° rotation between macrocyclic rings along the stacking c axis, and this stacking motif forms channels that the triiodides fill. The triiodide chain is ordered along the c axis, but each chain is disordered with respect to the others, causing a random potential within the macrocyclic chain. In all calculations reported here, the iodine atoms were placed in their average positions; no attempt was made to account for the iodine superlattice. In the study of the effect of ring rotation along the c axis, care was taken to ensure that the $4/m$ site symmetry of the phthalocyanine was retained.

The fractional point charge approximation, although fictional, has been useful[5,6] and is used here to assign the charges in eq 1. The q_i for the macrocycle are based on the Mulliken population analysis of the extended Hückel calculations of Schaffer et al.[7] and are given in Table I. The charges for $NiPc^+$ were found by assuming that the oxidized electron is removed from the highest occupied $a_{1u}(\pi)$ orbital. Since the $a_{1u}(\pi)$ orbital has nodes through all of the Ni–N planes, charge density on these atoms is unaffected by oxidation. For formal oxidation states between 0 and +1, a linear interpolation was used for each atom, $q(\rho) = (1 - \rho)q(0) + \rho q(1)$. The choice of charge model can be important; in the molecular metal TTF-TCNQ the Madelung energy was found to be very sensitive to the charge model employed.[5d] Although extended Hückel calculations are not the ideal choice for constructing a charge model, the results used here represent the best calculations on the entire metallophthalocyanine molecule and these results have been successful in explaining optical spectra and magnetic properties.[7]

Table I

atom[b]	ρ(NiPc)[a]	ρ(NiPc$^+$)[a]	atom[b]	ρ(NiPc)[a]	ρ(NiPc$^+$)[a]
Ni	+0.315	+0.315	C_3	−0.031	−0.002
N_1	−0.184	−0.184	C_4	−0.039	−0.022
N_2	−0.141	−0.141	H_3	+0.061	+0.061
C_1	+0.074	+0.150	H_4	+0.055	+0.055
C_2	+0.004	+0.008			

[a] Charges are given in units of $|e|$. [b] The numbering scheme is given by

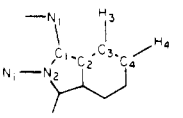

All other atoms are symmetry related in the D_{4h} point group.

The choice of charge on the iodine atoms is such that for a formal charge of $\rho+$ on each macrocycle a charge of $\rho-$ is assigned to each iodine atom. This simple model can be justified as a result of the disorder between iodine stacks within the NiPcI crystal.[2a] Each conducting stack does not experience a periodic potential from the iodine stacks, but rather an average over all counterions. This means that the charge on each iodine can be treated as the average of the entire crystal.

Results

One of the prime issues to be addressed is how the Madelung energy varies with the degree of charge transfer. Three different models for the conducting stack are used to probe this question. Case 1 is referred to as the Hartree–Fock (HF) limit;[11] in this case, each macrocycle is assigned a fractional oxidation state of $+\rho$. The charge on each atom of the macrocycle is found by linear interpolation of the end points given in Table I. Cases 2 and 3 are Wigner lattices. In each of these cases formally univalent macrocycles occupy ρ-lattice sites. For calculational purposes, the actual $NiPc^+$ occupation in each supercell is determined by minimizing the intrastack repulsion (as estimated by point charges). In case 2 the remaining lattice sites are left vacant (or equivalently, they are occupied by atoms with zero charge), while in case 3 these lattice sites are occupied by zerovalent macrocycles with an atomic charge distribution as shown in the NiPc column of Table I. A representative chain for $\rho = {}^1/_3$ is shown for each case in Figure 2.

For cases 1–3 the iodine stack is modeled by putting a $\rho-$ charge on each atom. This assumes that disorder exists between iodine chains. Thus, regardless of the chemical composition of the counterion stack, the disorder between chains causes the macrocyclic chains to experience an average charge due to each iodine site. For example, consider the hypothetical crystal $(NiPc^{+1/2})(I^{-1/2})$. Suppose the formally $I^{-1/2}$ stacks are chemically found to be ordered stacks of two I^- and one I_2. Assuming disorder between stacks, it follows that for a

(8) Evjen, E. *Phys. Rev.* **1932**, *39*, 675.
(9) Ewald, P. P. *Ann. Phys. (Leipzig)* **1921**, *64*, 253.
(10) (a) Born, M.; Huang, K. "Dynamical Theory of Crystal Lattices"; Oxford University Press: London, 1954. (b) Harris, F. E.; Michels, H. H. *Adv. Chem. Phys.* **1967**, *13*, 205.
(11) Soos, Z. G.; Ducasse, L. R.; Metzger, R. M. *J. Chem. Phys.* **1982**, *77*, 3036.

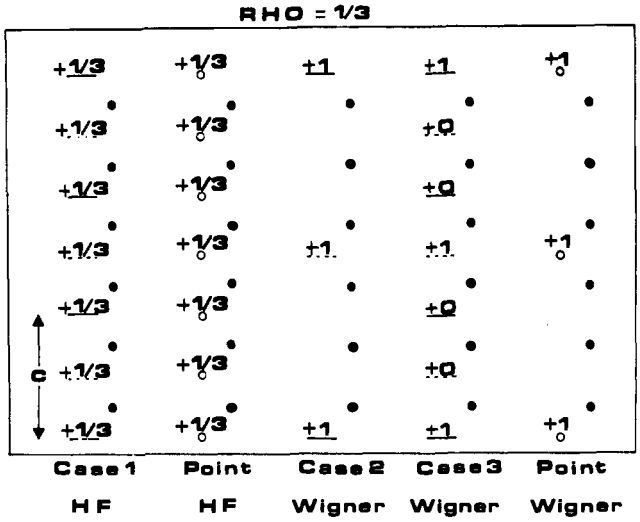

Figure 2. Representative chains for the models studied, $\rho = {}^1/_3$. Lines and open circles denote macrocycle positions (dashed lines indicate the 39.5° rotation) carrying the labeled charge. Closed circles denote iodine atoms, each assigned a charge of $-{}^1/_3$. Note that in the HF cases three units cells are shown, but for the Wigner cases, only one supercell is depicted.

given macrocycle the eight nearest-neighbor iodines have equal probability of being either I^- or I^0. In this case, then, the average charge on the nearest-neighbor iodine is $-{}^1/_2$. This type of disorder exists in the triiodide chains of NiPcI and is a reasonable model for other formal oxidation states as well. This model is similar to one used for the disordered ClO_4^- in Wurster's blue perchlorate.[5a]

Case 4 uses a Wigner lattice for both the macrocycle stack and the iodine stack. In this model the phthalocyanine chain is identical with that of case 2, while a 1− iodine is placed at the lattice sites nearest to the charged macrocycles, thereby maximizing the total Coulombic attraction. The charge at all other iodine sites is set to 0. Although this model does not appear to be physically justified, it allows a comparison to the more realistic uniformly charged iodine stack. This model also represents the situation in which the charges on the two stacks are highly correlated.

The charge-transfer dependence of the Madelung energy for NiPcI in the HF limit—case 1—is shown by the solid line in Figure 3. The points are calculated values, while the line represents the least-squares fit to the quadratic polynomial $E(\rho) = a + b\rho + c\rho^2$ ($a = 0.183$, $b = 1.202$, and $c = 0.334$, giving units of eV/molecule). As predicted by McConnell, Hoffman, and Metzger[12] (MHM) for the HF limit, no minimum exists in the range $\rho = 0$–1 (although extrapolation gives a minimum at $\rho \cong 1.8$); however, MHM predict that $E(\rho) \cong \rho^2 E(1)$, and this is clearly not the case for NiPcI. Also shown in Figure 3 are Madelung energies for a NiPcI lattice with point charges at the nickel ($\rho+$) and iodine ($\rho-$) sites (dashed line) and the Madelung energies for TTF-TCNQ as calculated by Metzger[5d] (dotted line). In contrast to NiPcI, both of these curves do follow the simple quadratic dependence of MHM. The difference in NiPcI results from the assumption that the oxidized electron is removed only from the $a_{1u}(\pi)$ orbital so that electron density at the major charge centers, the nodal metal and nitrogen atoms, is unaffected by oxidation. Effectively, this means that $E(\rho)$ is more appropriately viewed as

$$E(\rho) \cong q_1 q_2 E(1) = (a_1 + b_1\rho)(a_2 + b_2\rho)E(1) \qquad (2)$$

and while a_1 and $a_2 \cong 0$ for TTF-TCNQ, this is not the case for NiPcI. Clearly, eq 2 leads to the observed functional form. It is interesting to note that the NiPcI HF point lattice is strictly repulsive, indicating that the intrastack repulsion dominates the interstack attraction. The effect of the macrocycle is dramatic; the ligand serves to move a significant fraction of the positive charge ρ out to the periphery of the molecule and closer to the negative iodine, thereby greatly

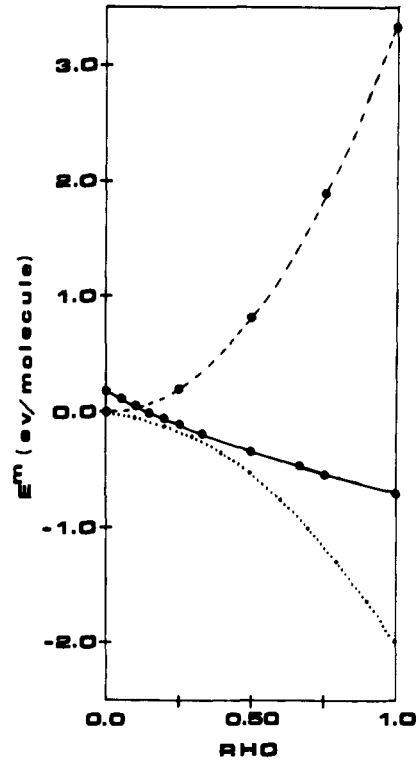

Figure 3. Charge-transfer dependence of the Madelung energy in the Hartree–Fock limit: (1) NiPcI, case 1 (solid line, $E = 0.183 - 1.202\rho + 0.334\rho^2$ eV/molecule); (2) NiPcI point lattice (dashed line, $E = 3.375\rho^2$ eV/molecule); (3) TTF-TCNQ (dotted line, $E = -0.0229 - 0.0611\rho - 1.918\rho^2$ eV/molecule). The points are the calculated values from which the least-squares fits were derived.

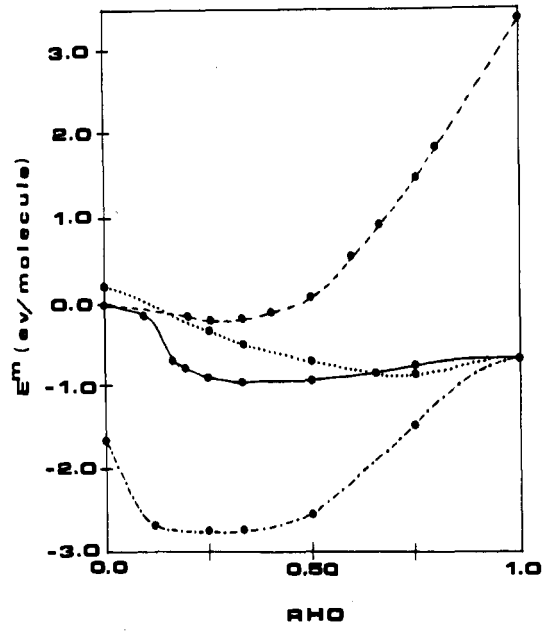

Figure 4. Charge-transfer dependence of the Madelung energy in the Wigner limit: (1) NiPcI, case 2 (solid line); (2) NiPcI, case 3 (dotted line); (3) NiPcI point lattice (dashed line); (4) NiPcI, case 4 (dot-dashed line). The points are the calculated values; the lines are drawn as guides for the eye.

(12) McConnell, H. M.; Hoffman, B. M.; Metzger, R. M. *Proc. Natl. Acad. Sci. U.S.A.* **1965**, *53*, 46.

enhancing the interstack attraction leading to $E^m < 0$ for $\rho > 0.15$ for case 1.

Figure 4 displays the charge transfer dependence of the Madelung energy for cases 2–4, the Wigner limit for NiPcI, and a Wigner point lattice. In contrast to the HF limit, these all show minima for $0 < \rho < 1$. The point lattice has a shallow, stable minimum at $\rho \cong 0.3$; at high values of ρ it mimics the HF point lattice. This demonstrates that the Wigner lattice decreases the intrastack repulsion by spreading the charges out along the chain but does not greatly alter the interstack attraction. As can be seen for cases 2 and 3, the effect of the macrocycle is to increase the interstack attraction, as in the HF limit, thus giving $E^m < 0$ for large ρ. Minima are at $\rho \cong 0.3$ for case 4, $\rho \cong 0.4$ for case 2, and $\rho \cong 0.7$ for case 3. Case 4 gives the most negative Madelung energy of any example discussed here, $E^m{}_{min} = -2.72$ eV/molecule; however, this does not approach the observed lattice enthalpy, $H_{lat} = -4.71$ eV/molecule.[4b] The correction between energy and enthalpy is of the order of RT and cannot account for the discrepancy. However, a simple analysis[4b] shows that the forces that bind the neutral constituents also provide more than half the lattice enthalpy in the charge-transfer complex. Thus, the "charge-transfer" portion of the lattice enthalpy is about −2eV/molecule, a value intermediate to cases 2 and 4. This suggests that some degree of charge correlation must exist between the cation and anion stacks in order to account for the observed lattice enthalpy.

The variation of the Madelung energy as a function of the angle of rotation between macrocycles along the stack is also studied. The angle of rotation, θ, is defined as the angle between the Ni–N_1 ($z = 0$) and Ni–N_1 ($z = {}^1/_2$) vectors when both are projected onto the same xy plane. When θ is varied, care is taken to ensure that the glide plane symmetry of the crystal is retained; i.e., the vector $(a/2, a/2, 0)$ always bisects θ. Values of θ were varied only from 0 to 60°; for $\theta > 60°$ neighboring chains of macrocycles begin to overlap and are not realistic structures unless the lattice parameters are enlarged. In all calculations the observed lattice constants were used. The results of these Madelung energy calculations are shown as the points in Figure 5 for cases 1 and 2 at the observed degree of charge transfer, $\rho = {}^1/_3$. Case 1 has a minimum at $\theta \cong 15°$, while case 2 is minimized at $\theta \cong 0°$. Both of these minima are well removed from the observed rotation of $\theta \cong 40°$. This clearly points out that the observed rotation between macrocycles is not electrostatic in origin but is a result of other steric and/or electronic energies in the system. It is found empirically that the calculated points can be reasonably well fitted to a function of the form

$$E^m(\theta) = a \sin^2 (\theta - \phi) + b \qquad (3)$$

as shown by the solid lines in Figure 5. The origin of this functional form, if not fortuitous, is unknown.

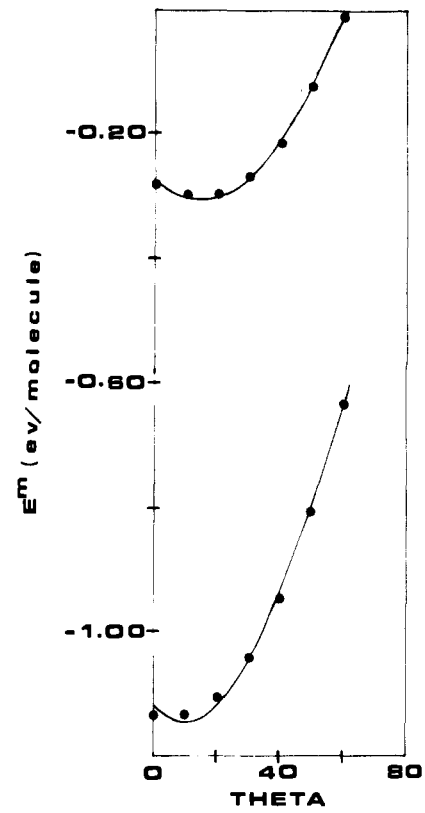

Figure 5. Madelung energy plotted as a function of the angle of rotation between nearest-neighbor macrocycles: upper curve, case 1, Hartree–Fock limit, $\rho = {}^1/_3$; lower curve, case 2, Wigner limit, $\rho = {}^1/_3$. Points are the calculated values; lines are the least-squares fit to $E^m(\theta) = a \sin (\theta - \phi) + b$. For case 1, $a = 0.586$, $b = 0.309$, and $\phi = 15°$, and for case 2, $a = 0.857$, $b = -1.147$, and $\phi = 10°$, giving E^m in units of eV/molecule.

Discussion

A Hamiltonian for the conducting chain in NiPcI would include the following terms: a site energy for the isolated donor ϵ_{NiPC}; a bandwidth along the chain axis, $4|t|$; an on-site electron–electron (Hubbard) repulsion, U; the Coulombic interactions previously calculated. An important parameter in this model is the ratio of the bandwidth to the on-site repulsion, $4|t|/U$.[13] A large bandwidth, $4|t| \gg U$, leads to charge delocalization along the chain and corresponds to the HF limit. In contrast, $4|t| \ll U$ tends toward charge localization in the chain and $|t| = 0$ is the strict Wigner limit. Magnetic susceptibility[2a] and the thermopower[4a] measurements on NiPcI suggest that $|t| \cong 0.10$ eV and the temperature dependences of these quantities imply that the HF limit is appropriate.

The nearest-neighbor Coulombic energy, E_{nn}, is important for determining the degree of electron–electron correlation along the conducting stack.[11] It is expected that for $|E_{nn}| > 4|t|$ nearest-neighbor correlations should be small and at the same time longer range and donor–acceptor correlations should exist;[11] that is, the crystal becomes more Wigner-like. For $|E_{nn}| < 4|t|$, the stack remains largely uncorrelated and approaches the HF limit. In the cases studied here, E_{nn} (using a simple classical calculation) varies significantly with the different charge models used for the conducting stack. Case 1, the charge-delocalized HF model, gives $E_{nn} = +0.22$ eV for $\rho = {}^1/_3$, or about half the estimated bandwidth. Thus, this model consistently represents a delocalized and uncorrelated limit. For case 2, $E_{nn} = 1.21$ eV for $\rho = {}^1/_3$ (where the nearest neighbors are spaced at intervals of $3c/2$), or about three times the estimated bandwidth. Here, the charges are localized with long-range correlations. As expected, cases 1 and 2 represent the extremes in charge localization and correlation models for the conducting stack. Case 3 is more subtle. There are two kinds of nearest-neighbor interactions: between a univalent macrocycle and a zerovalent macrocycle, $E_{nn}{}^{10}$; between two zerovalent macrocycles, $E_{nn}{}^{00}$. For the molecular charge distribution used here, both quantities are smaller than $4|t|$, $E_{nn}{}^{10} = -0.15$ eV and $E_{nn}{}^{00} = +0.12$ eV; so, by the simple criteria outlined above, the stack should approach the uncorrelated limit. In this case, however longer range Coulombic forces become important; for example, one of the third nearest-neighbor interactions for case 3 is identical with the nearest-neighbor repulsion of case 2, 1.21 eV, and this is the dominant interaction along the chain in case 3. This means that, although the stack is uncorrelated at short range, long-

(13) Shiba, H. *Phys. Rev. B: Solid State* **1972**, *6*, 930.

range correlations are important, and the chain retains its Wigner-like qualities.

Some degree of charge correlation between donor and acceptor stacks is necessary in order to account for the observed lattice enthalpy. The nearest-neighbor Coulombic attraction contributes about 60% of the total Madelung energy for the Wigner cases 2 and 4, whereas in the HF limit the nearest-neighbor attraction serves to reduce the total repulsion by about 25%. This makes the case 4 lattice significantly more stable than any of the others and serves to show that charge correlation between stacks can be used to account for the lattice energy, even though the actual model is physically inappropriate. The need for donor–acceptor charge correlations is at odds with the interpretations of the magnetic susceptibility and charge-transport experiments that point to the HF limit. Soos et al.[11] predicted that for some values of $4|t|$ (with respect to other crystal parameters) a system may appear to be simultaneously high correlated and uncorrelated; indeed, NiPcI must be such a system.

For a partially ionic state to exist in a given lattice, within the simplest contexts, there must be a stable minimum for some ρ in the electrostatic binding energy

$$E^{B}(\rho) = E^{m}(\rho) + \rho(I - A) \qquad (4)$$

where I is the ionization potential of the donor and A is the electron affinity of the acceptor. Evaluating eq 4 as a function of ρ for NiPcI is not straightforward because the electron affinity, A, has a ρ dependence. The model used to simulate the iodine charge lattice in the Madelung energy calculation is not appropriate for estimating the iodine electron affinities. For the Madelung energy calculations, the actual form of the iodine is unimportant since the average charge of each position in the iodine chain is sufficient; however, the detailed chemical distribution of the counterions is important for estimating the electron affinity. An instructive example is $\rho = {}^1/_3$. The observed chemical distribution is chains of I_3^-; however, another conceivable formulation is chains of alternating I^- and I_2. Yet, certainly the electron affinities of I^- and I_3^- are not the same.

When the simplifying assumption that all charge-bearing acceptors are iodide is employed, then $A = 3.12$ eV[14] and $I = 7.45$ eV,[15] and it is found that only case 4 of the models considered here gives a stable electrostatic binding energy for $0 < \rho < 1$. Cases 1 and 3 have minima at $\rho = 0$, case 2 has a minimum at $\rho \cong 0.2$, and case 4 has a minimum at $\rho \cong 0.1$; but, except for case 4, these minima have $E^B > 0$. Again, this shows the need for interstack charge correlation. Although the models for the Madelung energies are limited, it is apparent that more detailed values for the electron affinities are needed in order to reliably calculate E^B as a function of charge transfer. Because of this limitation, it cannot be ascertained if the observed ionicity of $\rho = {}^1/_3$ is the result of electrostatic or other forces. However, it seems clear that the stable $\rho = {}^1/_3$ state for NiPcI is not the result of a uniquely large electron affinity for triiodide, since Marks and co-workers have shown that $\rho \cong {}^1/_3$ is also the favored oxidation state even when the counterion is BF_4^- or PF_6^-.[4c]

The 40° rotation angle between macrocycles along the stack is not electrostatically favorable. The Madelung energies calculated here show that $\theta \sim 0$–10° is energetically preferred, but only by a small amount, approximately 0.1–0.2 eV depending on the charge model. Simple steric considerations suggest $\theta = 45°$ would be expected, so that neighboring benzo groups are as far apart as possible. Electronic interactions along the conducting stack are in accord with the Madelung energy; i.e., $\theta \sim 0°$. Simple overlap arguments lead to the conclusion that a wider band along the one-dimensional axis will be formed for smaller intermacrocycle rotation angles, and a wider band gives a more favored state. It appears, then, that no single predominant interaction can account for the observed rotation along the stacking axis.

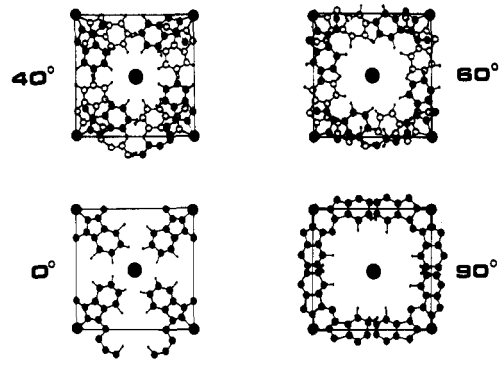

Figure 6. Macrocyclic packing around an iodine chain in NiPcI as projected onto the *ab* plane. Solid macrocycles are at $z = 0$, while the open ones are at $z = c/2$. The large solid circle represents the iodine chain at $(a/2, a/2, z)$. The diagrams depict the change in packing as a function of θ, the angle of rotation between macrocycles, without changing any other lattice parameters.

An analysis of the packing diagrams for NiPcI as a function of θ suggests that the observed rotation is a result of the most efficient packing motif for stacked metallophthalocyanines and iodine. Figure 6 shows a series of packing diagrams projected onto the *ab* plane as a function of θ. At $\theta = 0°$ the channel at $(a/2, a/2, z)$ marginally appears to be able to accommodate iodine. More importantly, in this configuration there are in-plane H–H contacts of 1.9 Å, nearly 0.5 Å less than a van der Waals contact, so that significant repulsion exists. Also note that the channels at $(a/2, 0, z)$ and $(0, a/2, z)$ could accommodate iodine chains, potentially introducing a disorder problem. As the macrocycles are rotated, the channel at $(a/2, a/2, z)$ becomes larger (hence accounting for the increasing Madelung energy) and near $\theta = 40°$ a "snug" fit for iodine is attained while at larger angles the cavity is large enough for the iodine to "rattle". With increasing θ the channels at $(a/2, 0, z)$ and $(0, a/2, z)$ close and the H–H repulsions are alleviated. However, by $\theta \sim 55$–60°, new in-plane H–H contacts are created, and at $\theta = 90°$ it is easily seen (Figure 6) that such a structure could not exist with the given lattice parameters. At either small or large angles the H–H repulsions could be alleviated by expanding the lattice constants, but this would also increase the separation between the cation and anion chains and thereby result in a decrease in the electrostatic attraction between the two types of chains, thus giving a more positive Madelung energy. At $\theta = 40°$ interatomic contacts between chains are all equal to or greater than van der Waals radii at a cost of perhaps 0.2 eV in electrostatic energy. Using the $\theta = 0°$ structure (which should be the most stable by electrostatic and electronic considerations) and expanding the a and b lattice constants so that the problematic H–H contacts are at van der Waals distances also only cost 0.1–0.2 eV in electrostatic energy, so that the potential disorder problem of the alternative channels must mitigate against this structure. These ideas could be tested by examining the structure of NiPcBr. Because of the smaller van der Waals radius of Br, the best packing for NiPcBr is predicted to be at $\theta \cong 35°$.

Finally, a comment about some of the other conducting NiPcX salts. X-ray powder diffraction studies on $NiPcI_x$, $0 < x < 4$, indicate that unique phases exist at $x \cong 1.0$ and x

(14) Sharpe, A. G. "Halogen Chemistry"; Gutmann, V., Ed.; Academic Press: London, 1967; Vol. 1.
(15) Eley, E. E.; Hazeldine, D. J.; Palmer, T. F. *J. Chem. Soc., Faraday Trans. 2* **1973**, *69*, 1808.

$\cong 3$. As in NiPcI, resonance Raman spectra for the $x \cong 3$ phase imply that the iodine is in the form of the chainlike triiodide. The $\theta = 0°$ structure (with the appropriate a and b lattice constants) could readily accommodate the increased iodine content of the $x \cong 3$ phase, and this seems to be a likely structure for this material. In contrast, the recently isolated PF_6^- and BF_4^- salts of $NiPc^{\rho+4c}$ would require $\theta > 40°$, on the assumption that the tetragonal lattice is retained. PF_6^- or BF_4^- situated at $(a/2, a/2, c/4)$ would require a larger volume than an iodine at the same site, and this could be most easily accomplished by a small, increased rotation of the macrocyclic rings. Of course, the Madelung energy for these materials could be significantly different from the iodinated crystal, largely depending on the degree of ordering in the counterion stacks, and this could require a substantially different structure to ensure stability. Currently, Madelung energy calculations for $NiPc(PF_6)_{0.36}$ and $NiPc(BF_4)_{0.34}$ are in progress.

Acknowledgment is made to the donors of the Petroleum Research Fund, administered by the American Chemical Society, for partial support of this research. The Academic Computing Center at the University of Rhode Island is also acknowledged for the generous allotment of computer time. I also thank Professor Brian Hoffman for helpful discussions and the reviewer for the suggestion to include case 4.

Registry No. NiPcI, 66625-96-5.

Contribution from the Departments of Chemistry, Queens College, City University of New York, Flushing, New York 11367, and University of Connecticut, Storrs, Connecticut 06268

Spectral and Photophysical Properties of Ruthenium(II) 2-(Phenylazo)pyridine Complexes

STEVEN WOLFGANG,[†] THOMAS C. STREKAS,*[†] HARRY D. GAFNEY,*[†] RONALD A. KRAUSE,[‡] and KIRSTEN KRAUSE[‡]

Received November 10, 1983

Resonance Raman and emission spectra are reported for a series of complexes $Ru(azpy)_2L_2^{n+}$ where azpy represents 2-(phenylazo)pyridine and L various monodentate ligands or a bidentate ligand. The resonance Raman spectra reveal a relatively localized MLCT excited state with large distortions of the azo N=N bond. Emission maxima for the luminescent complexes are significantly red shifted relative to those for other Ru(II) diimine complexes. These data along with previously measured electrochemical data suggest an energy level ordering in which the luminescent LMCT state is an exergonic oxidant and endergonic reductant. Quenching by a series of related oxidative and reductive quenchers is consistent with the calculated energetics of the photoinduced redox processes.

Introduction

The correlation between excited-state redox potentials and luminescence spectra has led to extensive investigations of Ru(II) polypyridine complexes.[1] During the last decade, a variety of substituted 1,10-phenanthroline (phen) and 2,2′-bipyridine (bpy) complexes have been prepared as a means to modify and tune the complexes' photophysical and photoredox properties.[2-4] In most instances, however, the perturbation introduced by the substituent is relatively small and the photoinduced properties of the substituted complexes remain essentially those of the parent analogue. Substantial modification of the excited-state properties apparently demands significant change in the bidentate, π-accepting ligands.

Recently, two of us described the preparation of a series of new Ru(II) complexes of the general formula $Ru(azpy)_2L_2^{n+}$ where azpy represents 2-(phenylazo)pyridine.[5] L represents a series of mono- and bidentate ligands of differing σ-donor and π-acid capabilities. The visible spectra of these complexes are dominated by intense visible transitions where the transition energy and an IR frequency assigned to the azo N=N stretch are functions of the π acidity of the coligands L. Our interest, however, was spurred by the luminescence and electrochemical behavior of these azpy complexes. When compared to those properties of the well-studied $Ru(bpy)_3^{2+}$,[6,7] the luminescence of the parent analogue, $Ru(azpy)_3^{2+}$, occurs at a lower energy and the complex has a larger oxidation potential, but a smaller reduction potential. This suggests an unusual energy level ordering in which the energy required to oxidize the ground state of $Ru(azpy)_3^{2+}$ exceeds the energy of the luminescent excited state. This inversion of the energy levels is quite different from that found with the polypyridine complexes, where the energy of the luminescent state generally exceeds that of the thermal redox steps and the excited state can act as an exergonic reductant or oxidant.[2] For the azpy complexes, however, the data suggest that reductive quenching of $Ru(azpy)_3^{2+}$ is exergonic whereas oxidative quenching of the complex is endergonic. For oxidative quenching to occur, the reduction potential of the quencher plus the excited-state energy must exceed the thermal oxidation potential of $Ru(azpy)_3^{2+}$. Consequently, reductive quenching by a quencher of known oxidation potential is also a means of bracketing the thermal oxidation potentials of the complexes, which are presently known only as lower limits.

To test these ideas based on luminescence–electrochemical energy changes, we have examined the photophysical properties and photoredox behavior of these $Ru(azpy)_2L_2^{n+}$ complexes. Resonance Raman spectra of the complexes confirm the MLCT character of the visible absorptions and suggest an excited-state configurations in which a significant portion of

[†] City University of New York.
[‡] University of Connecticut.

(1) Kalyanasundaram, K. *Coord. Chem. Rev.* **1982**, *46*, 161 and references therein.
(2) Lin, C. T.; Bottcher, W.; Chou, M.; Creutz, C.; Sutin, N. *J. Am. Chem. Soc.* **1976**, *98*, 6536.
(3) Berler, P.; von Zelewsky, A. *Helv. Chim. Acta* **1980**, *63*, 1675.
(4) Fabian, R. H.; Klassen, D. M.; Sonntag, R. W. *Inorg. Chem.* **1980**, *19*, 1977.
(5) Krause, R.; Krause, K. *Inorg. Chem.* **1982**, *21*, 1714.
(6) Paris, J. P., Brandt, W. W. *J. Am. Chem. Soc.* **1959**, *81*, 5001.
(7) Tokel-Takvoryan, N. E.; Hemingway, R. E.; Bard, A. J. *J. Am. Chem. Soc.* **1973**, *95*, 6582.

0020-1669/84/1323-2650$01.50/0